Int. J. Electrochem. Sci., 11 **(2016)** 5935 – 5951, doi: 10.20964/2016.07.48

International Journal of ELECTROCHEMICAL SCIENCE
www.electrochemsci.org

A Chemometrical Analysis of Voltammetric Data for Simultaneous Determination of Phenobarbital Sodium and Paracetamol Obtained at a Gold Electrode

Milka Avramov Ivić[1,*], *Jelena Antanasijević*[2], *Nemanja Trišović*[2], *Davor Antanasijević*[3], *Jelena Lović*[1], *Dušan Mijin*[2] *and Slobodan Petrović*[2]

[1] ICTM – Institute of Electrochemistry, University of Belgrade, Njegoševa 12, Belgrade, Serbia
[2] Faculty of Technology and Metallurgy, University of Belgrade, Karnegijeva 4, 11120 Belgrade, Serbia
[3] Innovation Center of the Faculty of Technology and Metallurgy, Karnegijeva 4, 11120 Belgrade, Serbia
[*]E-mail: milka@tmf.bg.ac.rs

Received: 24 March 2016 / *Accepted:* 5 May 2016 / *Published:* 4 June 2016

The electrochemical behavior of phenobarbital sodium (PBS), paracetamol (PCM) and their binary mixtures was investigated using cyclic voltammetry (CV) and square wave voltammetry (SWV) at a bare gold electrode in a 0.05 M bicarbonate solution. A calibration curve of PBS obtained by SWV had two linear ranges, from 1.0 to 3.0 μM and from 5.0 to 35.0 μM with a limit of quantification (LOQ) of 0.62 μM and a limit of detection (LOD) of 0.19 μM, while a calibration curve of PCM was determined within the range from 10.0 to 50.0 μM with a LOQ of 8.53 μM and a LOD of 2.56 μM. Both drugs underwent oxidation by irreversible, diffusion controlled process. The SW voltammograms of the drug mixtures produced complex, overlapping profiles and a chemometric method was applied for their decomposition. Two different artificial neural network (ANN) architectures, namely back-propagation neural network (BPNN) and general regression neural network (GRNN) were employed for the simultaneous prediction of the concentrations of the drugs in a synthetic sample. The BPNN model had higher accuracy (mean absolute percentage error values were in the range of 3.6–8.4%) and thus it can be used for the simultaneous determination of PBS and PCM.

Keywords: phenobarbital, paracetamol, voltammetry, chemometrics

1. INTRODUCTION

As the oldest and the safest anticonvulsant drug, phenobarbital (PB) is used principally in the management of tonic-clonic and partial seizures [1]. Its precise mechanism of action is still unknown,

but is thought to involve blockade of sodium channels and enhancement of GABA-mediated inhibitory transmission [2]. The drug is used for routine sedation or to relieve anxiety and provide sedation preoperatively [1]. PB may also be used for short-term treatment of insomnia [3].

Many requests for the determination of the anticonvulsant drugs arise as a result of problems in the patient management. PB has a narrow therapeutic range, so its concentration need to be monitored in order to adjust the dose to the optimal level for effective therapeutic control but with minimal side effects such as neurological toxicity [4]. The drug is frequently used in combination with antipyretics, such as paracetamol (PCM), since its presence reduce the recurrence risk of simple febrile seizures [5]. PB with minimal neurological toxicity in combination with PCM is frequently used in pediatrician praxis in order to avoid and minimize high fiver convulsions [4]. Therefore, multiple assays for the routine measurement of these two drugs, with high sensitivity and selectivity, are needed and it was the reason for the choice of PB and PCM as the mixture for the simultaneous determination.

Several methods that allow the simultaneous determination of PB and PCM have been reported in the literature, including spectrophotometry [6,7], high-performance liquid chromatography (HPLC) [8] and electrochemistry [9,10]. As rapid, simple, sensitive, selective and low cost, electrochemical methods are more favorable than the chromatography and spectrophotometry, which require a prior separation steps and tedious analytical process during analysis, the use of organic solvents, thereby generating high amounts of waste, time-consuming derivatization steps and high implementation costs [11–13]. Differential pulse voltammetry (DPV) has been successfully applied for the determination of PB and PCM in pharmaceuticals. Ni *et al.* [9] have investigated their electrochemical behavior at a glassy carbon electrode. Due to the overlapping oxidation peaks of these two drugs, the interpretation of the complex voltammograms of a mixture has been achieved with the aid of chemometric methods. Raoof *et al.* [10] have prepared a modified electrode by simple incorporation of multi-walled carbon nanotube (MWCNT) and Pt-nanoparticles into a paste matrix. The DPV response of a drug mixture reveals two well-distinguished oxidation peaks, corresponding to the oxidation of PB and PCM, which allow their individual determination. PCM was the subject of the electroanalysis on modified gold electrode surfaces [14,15].

Because the electrode response can perform in a non-linear way, artificial neural networks (ANNs) as non-linear estimators, among other chemometric methods, are widely used for the evaluation of electrochemical signals [16,17]. ANNs are non-parametric regression method that can fit non-linear relationship between two or multiple variables by learning from a set of examples and generalize this knowledge to the new set of data. Considering that ANNs can perform well in the presence of complex, noisy and/or incomplete data, they are especially useful for the simultaneous prediction of several components in mixtures, which have complicated voltammetric responses because of highly overlapping peaks or reactions between components [18–21].

The aim of the present study is to analyze electrochemical behavior of PBS, PCM (Fig.1) and their mixtures by cyclic voltammetry (CV) and square wave voltammetry (SWV) using a bare gold electrode in 0.05 M $NaHCO_3$; pH = 8.4. In addition, the simultaneous determination of PBS and PCM using SWV data and ANN, as a chemometric method for the decomposition of the voltammograms, is described. Two different feed-forward supervised ANN architectures, namely back-propagation neural network (BPNN) and general regression neural network (GRNN) have been used, and compared, for

the simultaneous prediction of the concentrations of PBS and PCM in a synthetic sample. Following the proposed method, these two drugs can be determined directly, simultaneously and rapidly from the SW response of a given sample.

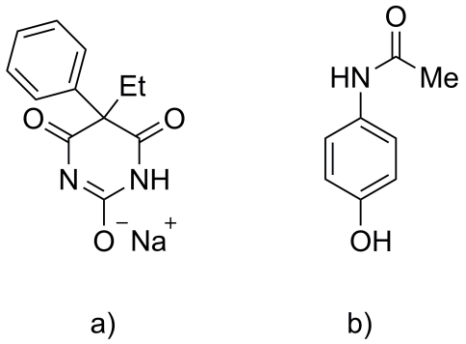

Figure 1. Chemical structures of: a) phenobarbital sodium and b) paracetamol

2. EXPERIMENTAL

2.1. Reagents

All reagents were purchased from Sigma Aldrich and were used without any further purification. For all experiments, chemicals and solvents of analytical reagent grade or better were used. Deionized water was obtained from a Milipore Waters Milli-Q purification unit. Stock solutions of each compound (2.0 g dm^{-3}) were prepared in methanol by weight and direct dilution. Appropriate aliquots of the stock solution were added into the electrolyte 0.05 M $NaHCO_3$ in order to obtain target concentrations, whereby the total concentration of methanol did not exceed 1 %.

2.2. Apparatus and preparation of electrode surfaces

Standard equipment has been used for the cyclic voltammetry measurements and the three electrode electrochemical cell was described in detail previously [22]. Polycrystalline gold (bare gold, surface area 0.07 cm^2) which served as the working electrode, was polished with diamond paste, cleaned with a mixture of 18 MΩ deionized water and sulfuric acid and further cleaned with 18 MΩ deionized water in an ultrasonic bath. A gold wire was used as the counter electrode and a saturated calomel electrode (SCE) as the reference electrode. All the potentials are given *vs*. SCE. Prior to each experiment working electrode was checked by cycling the potential scan between –450 and 1100 mV in supporting solution (0.05 M $NaHCO_3$; pH= 8.4) at the scan rate of 50 mV s^{-1} until the unchanged CV characteristics for Au electrode were obtained. After that the electrode was transfer to the electrochemical cell containing analytes and electrochemical measurements were performed. Between two consecutive concentrations the gold electrode was cleaned as described. The electrolytes have been deoxygenated by purging with nitrogen. All the experiments have been performed at room

temperature using PGZ 402 Volta Lab (Radiometer Analytical, Lyon, France). Square wave voltammetry measurements were carried out using pulse size 25 mV; frequency: 10 Hz; step size: 5 mV and scan rate 50 mV s^{-1}, with the accumulation time of 0.2 s at 0.0 mV.

2.3. Preparation of mixtures

Standard solutions (Table 1) were prepared by mixing aliquots of different concentrations of PBS and PCM into the electrolyte 0.05 M $NaHCO_3$. The concentration of samples 1–10, which were used as the training dataset for the development of ANN models, was established through an experimental design for two factors, "central composite" of type "2^2 + star", rotatable, and with two central points in the concentration range from 1.0 to 3.0 μM for PBS and 40.0 to 80.0 μM for PCM. Samples 11–17 and 18–22 were designed to obtain the validation and test dataset, respectively. The concentration of samples used as the validation and test data were selected in the same concentration range as in case of training data.

Table 1. Concentration of PBS and PCM used as output data in the development of ANN models

Dataset	Sample	PBS (μM)	PCM (μM)	Dataset	Sample	PBS (μM)	PCM (μM)
Training	1	2.0	80.0	Validation	11	1.0	40.0
	2	2.0	40.0		12	1.0	70.0
	3	3.0	60.0		13	1.5	60.0
	4	2.0	60.0		14	2.0	50.0
	5	2.5	70.0		15	2.5	40.0
	6	2.5	50.0		16	3.0	40.0
	7	1.0	60.0		17	3.0	70.0
	8	1.5	50.0	Test	18	1.0	50.0
	9	1.5	70.0		19	1.5	40.0
	10	2.0	60.0		20	2.0	70.0
					21	2.5	60.0
					22	3.0	50.0

2.4. ANN architectures

2.4.1. Back-propagation neural network

Back-propagation neural network (BPNN) is a standard feed-forward ANN architecture consisted of three layers of neurons: an input layer, a hidden layer and an output layer (Figure 2). The number of neurons in the input (N_i) and output (N_o) layer is equal to the number of input and output parameters that are used in the BPNN model, while the number of neurons in the hidden layer (N_h) is often determined using following equation [23]

$$N_h = \frac{(N_i + N_o)}{2} + \sqrt{n_{tr}} \quad (1)$$

where n_{tr} is the number of training samples.

The neurons from one layer are connected only with the neurons from the immediate next layer and the strength of those connections is quantified with a weight factor (W_{ij}). During the BPNN training the weights are iteratively adjusted, using the back-propagation algorithm [24], with aim to minimize the sum of squared difference between the known output and the predicted one. In each iteration the correction of weights (ΔW_{ij}) was performed using following equation

$$\Delta W_{ij(n+1)} = \eta \delta_j Y_j + \alpha \Delta W_{ij(n)} \quad (2)$$

where Y_j is the output of neuron j in the hidden layer, η is the learning rate, δ_j is the error term, α is the momentum and n is the iteration number. The weighted sum of linearly scaled inputs is transformed to the neuron output using the sigmoid activation function.

2.4.2. General regression neural network

A general regression neural network (GRNN) is also a feed-forward neural network with supervised training based on the nonlinear regression theory [25]. It consists of four layers, namely an input layer, a pattern layer, a summation layer and an output layer (Figure 2). The number of neurons in the GRNN layers is determined by the number of input/output parameters and the number of training samples used for model training: the input/output layer has one neuron for each input/output parameter, the pattern layer has one neuron for each training sample, while the summation layer has one neuron for each output variable, plus one. As it is indicated in Figure 2, the summation layer has two different types of neurons, the summation neurons (S_1 and S_2) and a single division neuron (D). The summation neurons S_1 and S_2 compute the sum of the weighted outputs of the pattern layer, while D calculates the un-weighted outputs of the pattern neurons [26]. Each of the GRNN output neurons is connected only to its corresponding S and to the D neuron and there are no weights in these connections.

In contrast to the BPNN, the weights in GRNN architecture are defined using one-pass algorithm that sets the weights between the input and pattern layer (W_{ij}) to the value of input parameters (from the training dataset), while the weights between the pattern layer and summation neurons (W_s) are set to the value of corresponding output parameters (from the training dataset).

The GRNN measures the distance (Dj) of the training samples in N-dimensional space, and then the calculated Dj is processed in the pattern layer using an exponential activation function [27]. As it is presented in Figure 1, during the GRNN training, only one parameter, called the smoothing factor (σ), need to be adjusted. The smoothing factor represents the width of the calculated Gaussian curve for each probability density function [25]. In the present study, the optimal value of smoothing factor is determined using a genetic algorithm (GA). More details on the GA and its application for GRNN training can be found elsewhere [28,29].

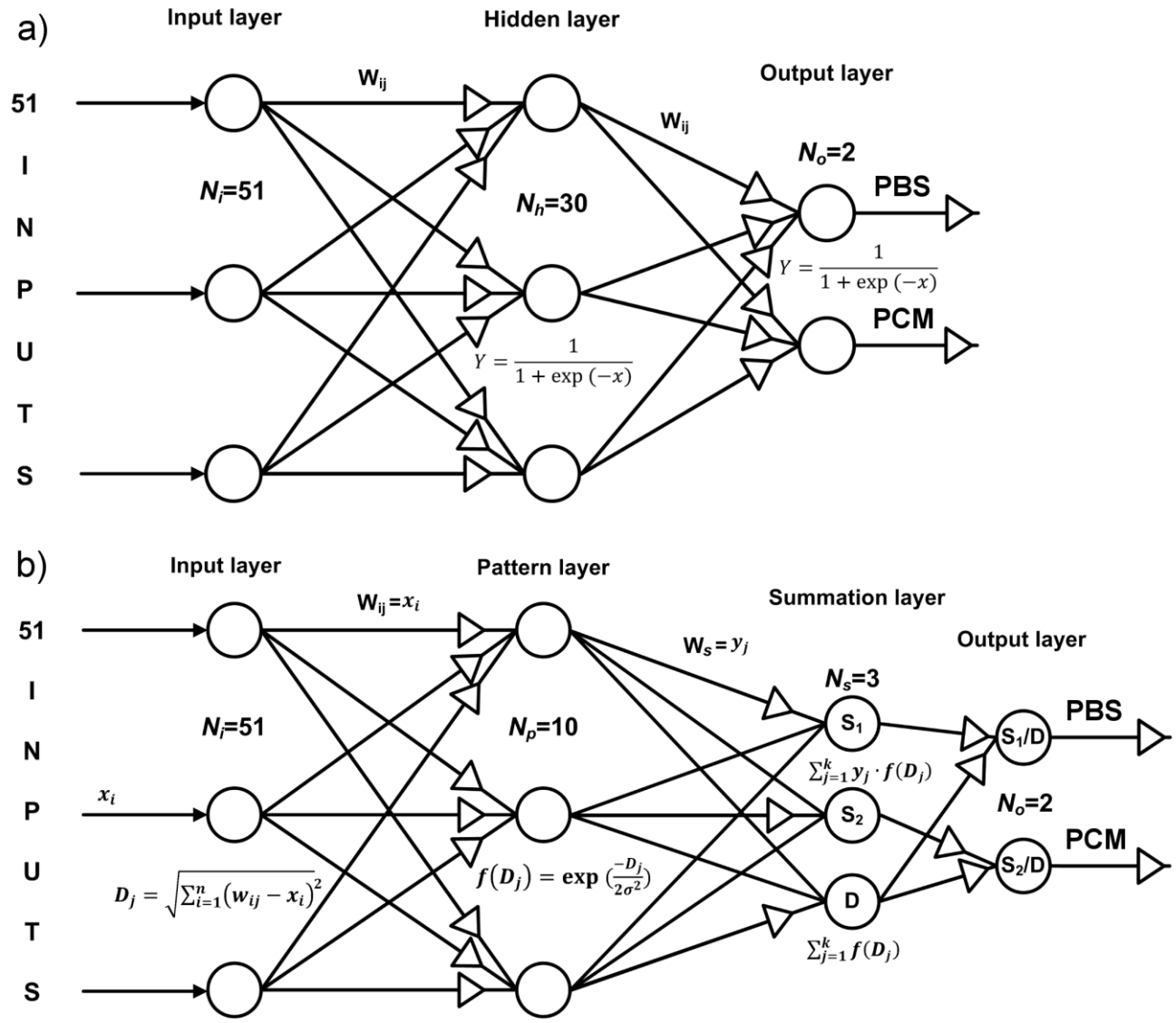

Figure 2. Schematic representation of the ANN architectures used in this study: a) BPNN and b) GRNN.

3. RESULTS AND DISCUSSION

A polycrystalline gold electrode was selected as the optimal working electrode for the examination of the phenobarbital and paracetamol because it is defined with a quite reproducible voltammograms enabling that all the electrochemical reactions at electrode surface could be attributed to the studied molecules [30]. Gold electrode is prepared by mechanical polishing with diamond paste, followed by cleaning. The surface roughness after "rough" mechanical polishing can be recognized only on the nanoscale. The voltammograms are reproducible under the described experimental conditions [31].

3.1. Cyclic voltammetry characterization of the drugs and their binary mixtures

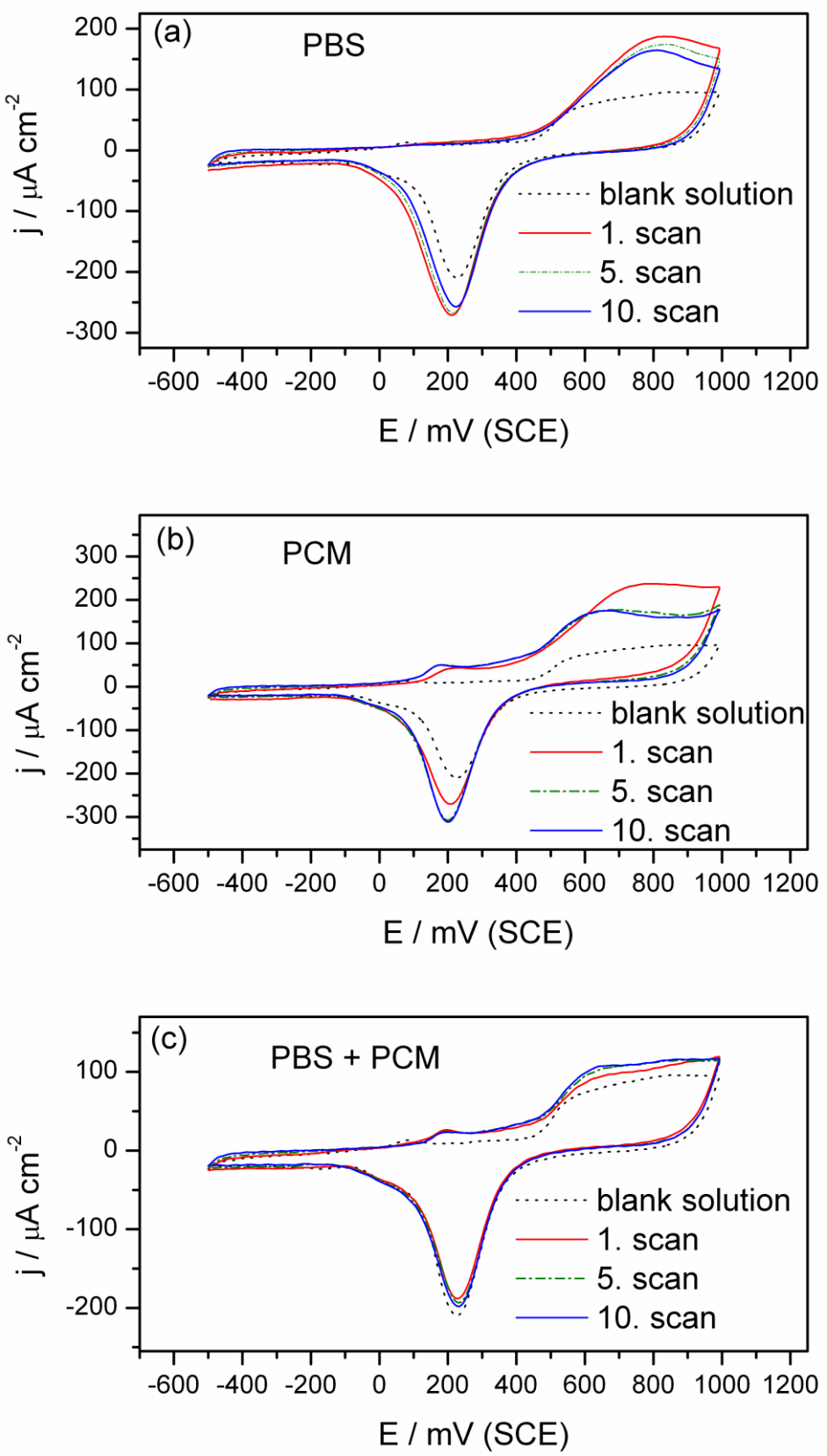

Figure 3. CVs obtained on gold electrode using 0.05 M $NaHCO_3$ in the presence of: a) PBS (45 µM), b) PCM (100 µM), c) binary mixture of PBS (1 µM) and PCM (50 µM) at scan rate 50 mVs^{-1}.

To analyze the electrochemical behavior of the investigated drugs on a bare gold electrode, CV measurements have been firstly performed. The cyclic voltammograms of PBS, PCM and their mixture (the first ten continuous scans) are shown in Figure 3. Compared to the clean electrode, PBS exhibits a well-defined oxidation reaction in the area of the gold oxide formation (Fig 3a). A decrease in the oxidation peak current after successive scans could be attributed to the presence of PBS intermediates formed during the oxidation. The gold oxide reduction peak is slightly decreased and shifted to more negative potentials upon further scans according to the reduction of the oxidized products formed in the forward scans. Electrochemical oxidation of phenobarbital and paracetamol at the glassy carbon electrode were found to be pH dependent [9]. On gold electrode it is found as well as on glassy carbon [9] that in an acidic medium, the amide group in PCM and PBS reacts with a proton to form salts, which are generally difficult to oxidize. However, the amide group will convert into the corresponding enol form in an alkaline medium and can be further oxidized. Thus, for phenobarbital, the peak current increases somewhat with increasing pH.

In a moderately alkaline medium (pH 8.4), it is the enol form of the barbituric moiety in PBS that reacts and as its concentration in the equilibrium mixture is depleted, more of the keto form changes over to the enol. A decrease in the oxidation peak current after successive scans could partly be attributed to the slow conversion between isomers of barbituric moiety in PBS [15]. Using the different electrolytes (phosphate buffers) at different pH values (5.5–9) showed the lower oxidation ability of PBS and PCM than was obtained by using 0.05 M $NaHCO_3$. A similar situation was observed while investigating the electrochemical behavior of phenytoin and related cyclic amides on a gold electrode [22].

Regarding the electrochemical behavior of PCM, the first small, sharp oxidation peak appears at the potentials more negative than the gold oxide is formed, i.e. at 200 mV. The second one, more developed and with much higher currents, is observed at 600 mV in the area of the gold oxide formation (Fig. 3b). The current of the peak at 600 mV decreases from the first to the fifth scan while the peak at 200 mV remains almost unchanged. The gold oxide reduction peak is shifted to the more negative potentials and increases upon further scans. This indicates the significant involvement of the species formed in a forward scans in the gold oxide reduction.

In Fig. 3c are displayed the voltammograms obtained by the mixture of PBS and PCM. A considerable overlap of the peaks in the region from 450 to 1000 mV is evident, while the oxidation peak at 200 mV for PCM can still be detected. Comparing to Figs. 3a and 3b, the lower reaction currents observed in Fig. 3c are most probably the consequence of the competitive adsorption of PBS and PCM.

Figures 4, 5 and 6 demonstrate the CVs on Au at different scan rates (v) in 0.05 M $NaHCO_3$ containing 15 μM PBS, 50 μM PCM and their mixture (1 μM PBS + 50 μM PCM), respectively. It is obvious that the currents become higher with the increased scan rate. In all three figures, the relationship between peak current and $v^{1/2}$ is displayed (inset a) showing linearity and indicating that the PBS and PCM oxidation is diffusion controlled processes. The oxidation of their mixture underwent the same process.

According to Bard and Faulkner, the peak potential decreases with the increasing scan rate, and a straight line relationship can be observed from the dependency of the peak potentials on ln of scan

rates (in the all three Figures, inset b), suggesting that PBS, PCM and their mixture underwent to an irreversible electrode process [32].

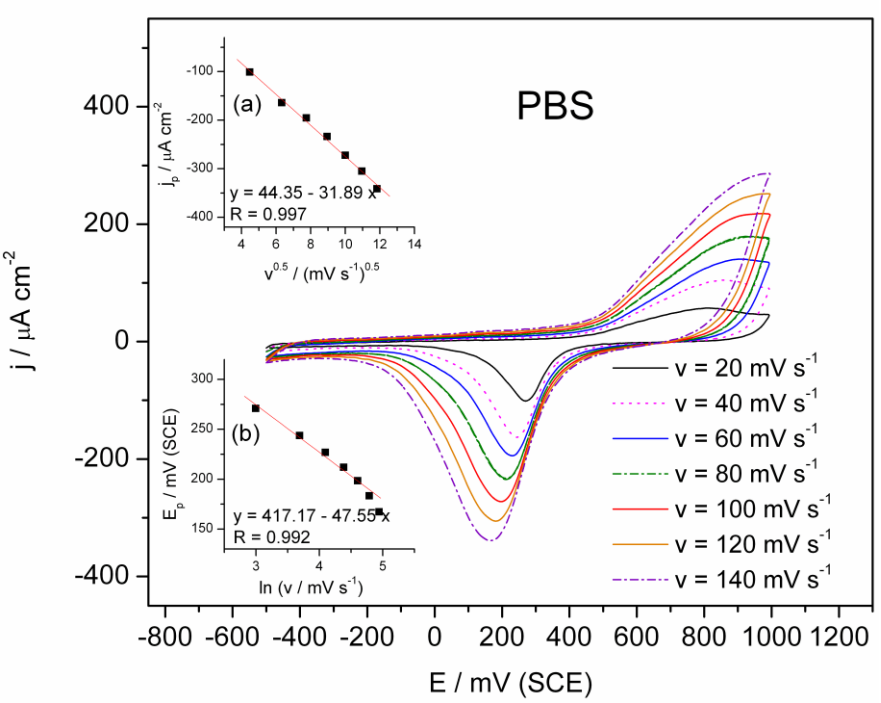

Figure 4. CVs of 15 µM PBS on gold electrode using 0.05 M $NaHCO_3$ for scan rates: 20, 40, 60, 80, 100, 120 and 140 mV s^{-1}. Insets: a) plots of peak current density *vs*. $v^{1/2}$ and b) peak potential shift *vs*. ln of scan rates.

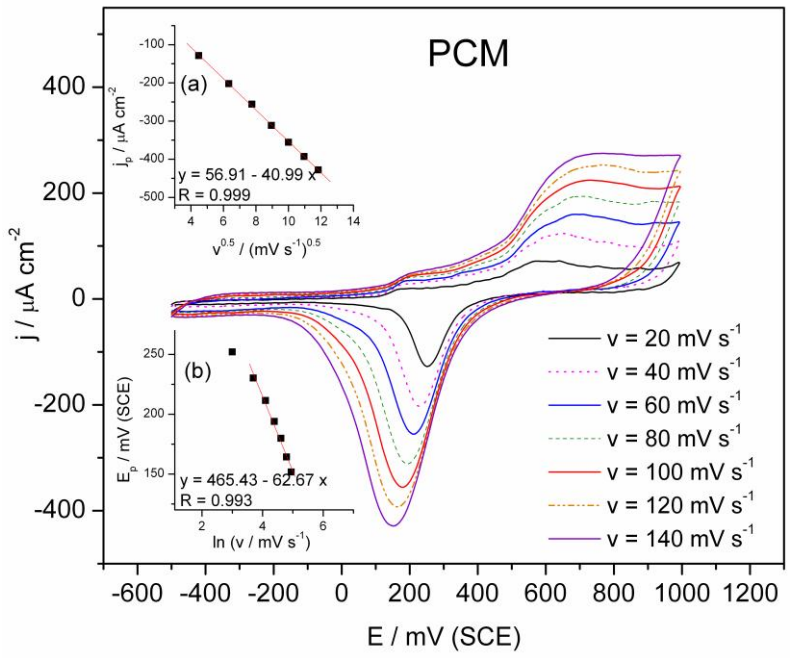

Figure 5. CVs of 50 µM PCM on gold electrode using 0.05 M $NaHCO_3$ for scan rates: 20, 40, 60, 80, 100, 120 and 140 mV s^{-1}. Insets: a) plots of peak current density *vs*. $v^{1/2}$ and b) peak potential shift *vs*. ln of scan rates.

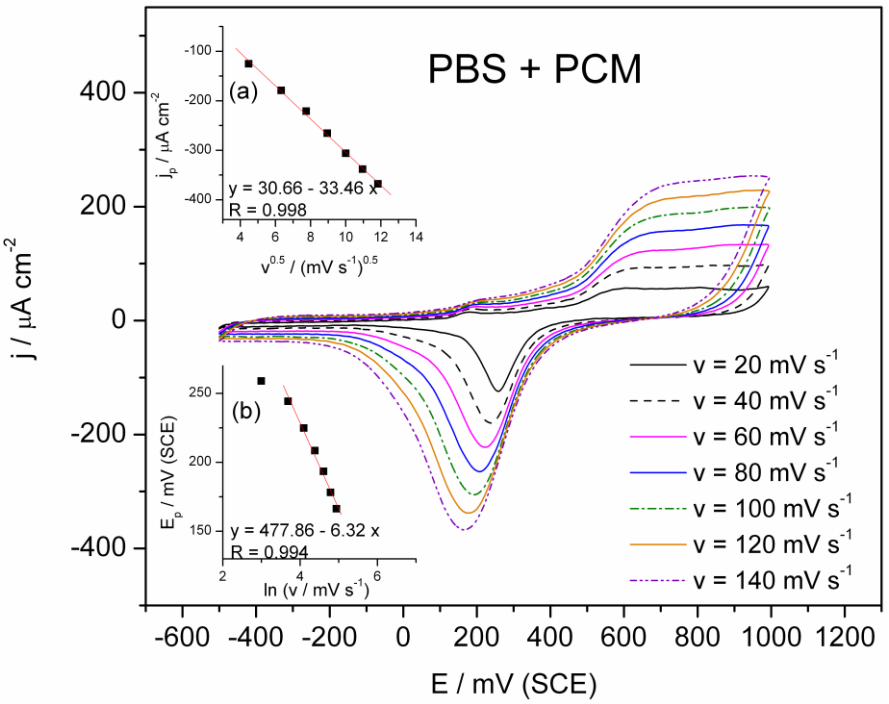

Figure 6. CVs of 15 μM PBS + 50 μM PCM on gold electrode using 0.05 M $NaHCO_3$ for scan rates: 20, 40, 60, 80, 100, 120 and 140 mV s^{-1}. Insets: a) plots of peak current density *vs*. $v^{1/2}$ and b) peak potential shift *vs*. ln of scan rates.

The Laviron's theory for irreversible processes was applied in order to calculate the number of electron transferred and the heterogeneous electron-transfer rate constant (k^0) [33]:

$$E_p = E^0 + \left(\frac{2.303RT}{\alpha nF}\right)\log\left(\frac{RTk^0}{\alpha nF}\right) + \left(\frac{2.303RT}{\alpha nF}\right)\log \nu \qquad (3)$$

where E^0 is the formal potential, T is the temperature in degrees Kelvin (298 K), α is the transfer coefficient, k^0 is the rate constant for the interfacial electron transfer process (per second), n is the number of electrons transferred in the rate determining step, v is the scan rate, F is the Faraday constant (96480 C mol^{-1}), and R is the universal gas constant (8.314 K^{-1} mol^{-1}).

Thus, the value of *αn* is easily calculated from the slope of Ep *vs*. log v. For PBS, PCM and their mixture the value of slope is 137.5, 144.3 and 136.4, respectively. Further, the number of electron (n) transferred in the electrooxidation of PBS and PCM was calculated to be approximately equal to 1 since the value of α is 0.5 for an ideal diffusion-controlled electrode process. The value of k^0 can be determined from the intercept of the previous plot if the value of E^0 is known. The value of E^0 can be obtained from the intercept of Ep *vs*. v curve and the value for PBS, PCM and their mixture is 273.7, 264.1 and 271.8 mV, respectively. From this k^0 was calculated to be 0.713 s^{-1} for PBS, 0.794 s^{-1} for PCM and 0.66 s^{-1} for their mixture. Somewhat higher rate constant for the interfacial electron transfer process was obtained for PCM suggesting faster electron transfer between PCM and gold electrode surface.

3.2. Squre wave voltammetry of the individual drugs and their binary mixtures

The obtained CV results indicate that SWV technique should be tested for the simultaneous determination of PBS and PCM. The SWV responses of the individual drugs are shown in Figures 7 and 8. In the SW voltammogram of PBS, one well developed and sharp oxidation peak appears at 500 mV and exhibits the linear dependency on the lower concentration in the range from 1.0 to 3.0 μM (inset in Fig. 7a). Another set of higher concentrations is tested (from 5.0 μM to 35.0 μM PBS) and the same voltammetric response is obtained as is presented in Fig. 7b. A linear dependency of peak currents on the concentration is given in inset in Fig. 7b. Comparing the calibration curves for two concentration sets, it can be seen that the higher slope obtained for the set from 1.0 to 3.0 μM indicate the higher sensitivity of a gold electrode in determining PBS in this concentration range.

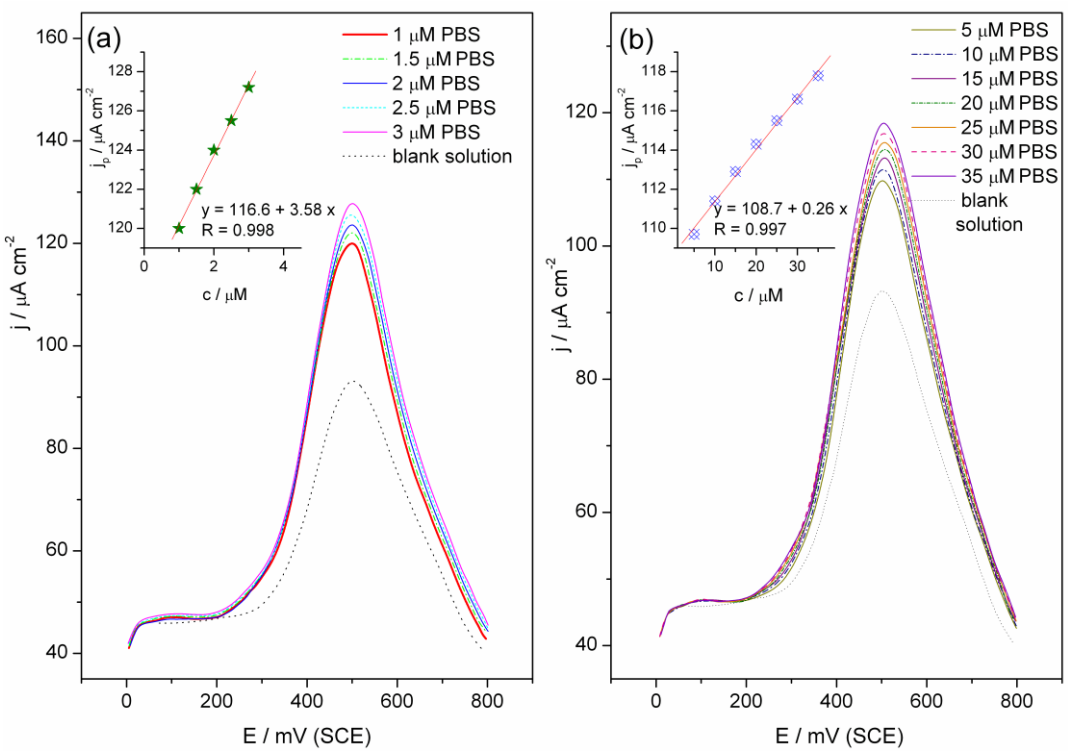

Figure 7. SW voltammograms obtained with the Au electrode using 0.05 M $NaHCO_3$ for a set of: a) lower concentrations of PBS; Inset: linear dependency of anodic peak currents *vs.* concentration of PBS, and b) for a higher concentrations of PBS, Inset: linear dependency of anodic peak currents *vs.* concentration of PBS.

In the case of PCM, the SWV response exhibits one smaller oxidation peak from 50 to 300 mV and one dominant oxidation reaction from 300 to 800 mV with the current maximum at 500 mV (Figure 8). The dominant peak currents increase linearly with increasing the concentration in the range from 10.0 to 50.0 μM (Inset in Fig. 8a) and afterwards they decrease gradually as the drug concentration continues to increase. As is presented in Fig. 8b, on the other side, the peak currents of the smaller oxidation reaction at 160 mV exhibit a linear dependency on the concentration in the range from 40.0 to 100.0 μM (Inset in Fig. 8b).

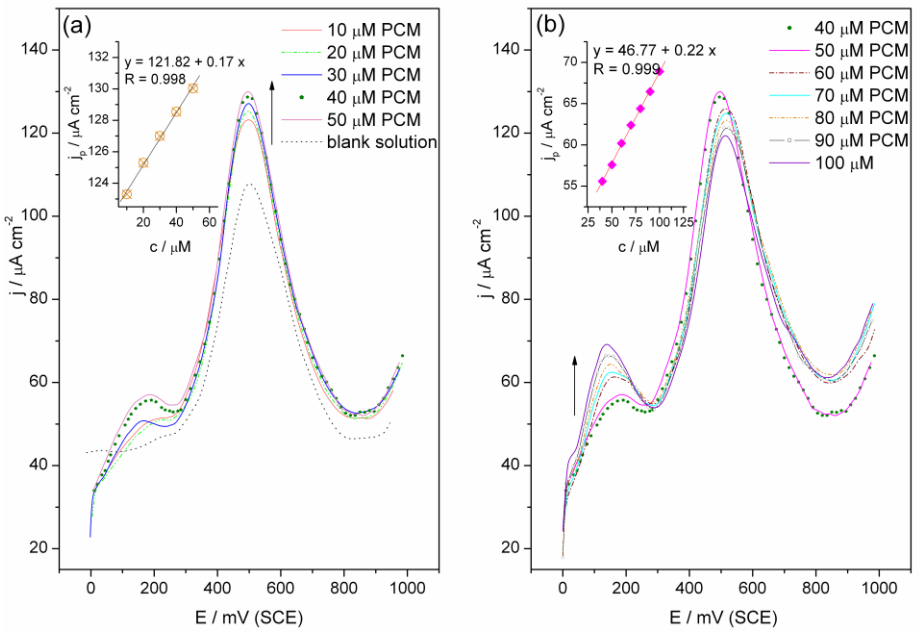

Figure 8. SW voltammograms obtained with the Au electrode using 0.05 M $NaHCO_3$ for a set of: a) concentrations of PCM; Inset: linear dependency of anodic peak currents *vs*. concentration of PCM, and b) concentrations of PCM, Inset: linear dependency of anodic peak currents *vs*. concentration of PCM.

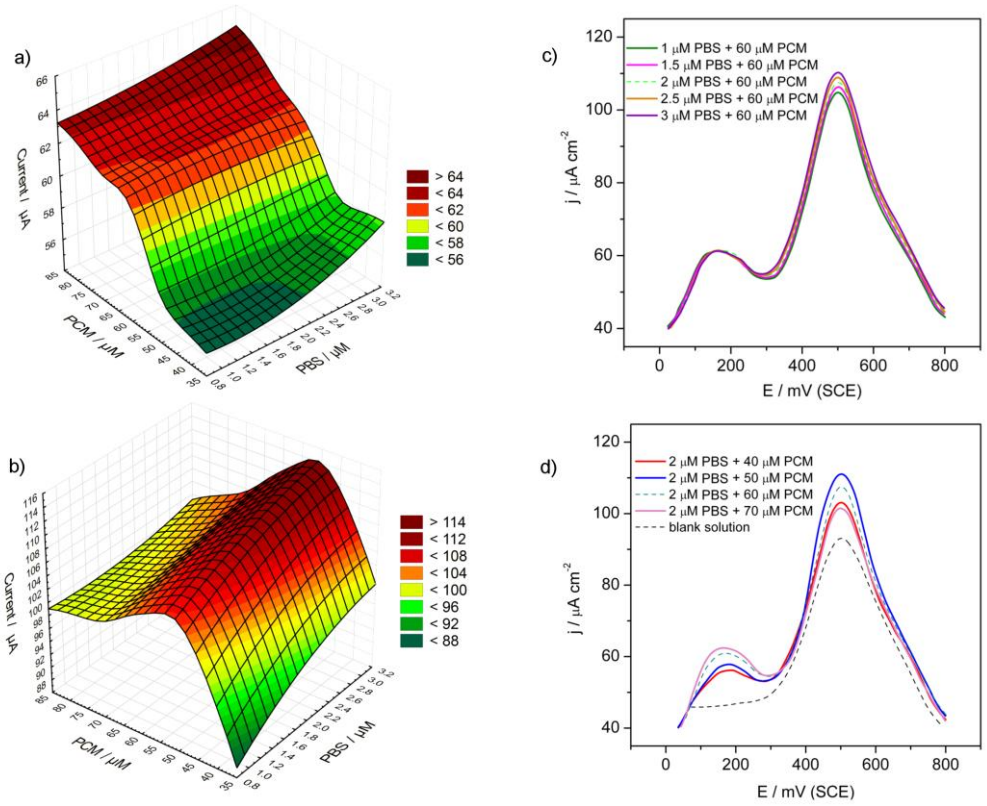

Figure 9. Response surfaces obtained for the binary mixtures: a) the peak currents at potential 165 mV and b) 500 mV. SW voltammograms of the binary mixtures containing: c) 60 μM PCM and different concentrations of PBS (1.0–3.0 μM) and d) 2.0 μM PBS and different concentrations of PCM (40–70 μM).

The limit of detection (LOD) and the limit of quantification (LOQ) are estimated using the statistical method described by Miller and Miller [34], which is suggested to be used for the electroanalytical work [36]:

$$LOD = \frac{3\sigma_a}{b} \quad (4)$$

$$LOQ = \frac{10\sigma_a}{b} \quad (5)$$

where b is the slope and σ_a is the standard deviation of the intercept of the calibration curve. The LOD were found to be 0.19 and 2.56 μM for PBS and PCM, respectively. The LOQ were found to be 0.62 and 8.53 μM for PBS and PCM, respectively. The obtained detection limit for PBS and PCM is comparable with values reported in the literature [9,10].

The SW voltammograms and the representation of the response surfaces (measured currents) obtained for the mixture samples are shown in Figure 9.

The SWV of the binary mixtures of PBS and PCM reveals two well-resolved oxidation reactions with the current maximums at 160 and 500 mV. A broad peak at 500 mV evidently results from the overlap of the voltammetric responses of the individual drugs in the potential range of the gold oxide formation (Fig. 7 and 8). As can be seen, the oxidation peak currents at 500 mV increase as the concentration of PBS increases at a fixed concentration of PCM. On the other side, keeping the concentration of PBS constant, the oxidation peak current firstly increases with increasing the concentration of PCM, reaches the maximum at ca. 55.0 μM and then decreases as the concentration of PCM continues to increase. Interestingly, the peak current at 500 mV of the binary mixtures is lower than the peak currents of the individual drugs at the same concentrations, probably due to their competition for active sites on the electrode surface. A small peak of PCM at 160 mV is also observed in the SW voltammogram of the binary mixtures as shown in Fig. 9. The peak current increases with increasing the concentration of PCM in the range from 55.0 to 80.0 μM, while it does not meaningfully change with the change of the concentration of PBS.

3.3. ANN modeling

Because of the overlapping of the voltammetric responses of the individual drugs in their mixtures, two chemometric methods were used for the construction of calibration models based on SWV results. The values of the measured current taken for the corresponding potentials regularly distributed (15 mV) in the measured potential range (45 to 795 mV) were used as inputs. Therefore, from each measured voltammogram, 51 current values were obtained and fed as an input vector into the ANN. The concentrations used and datasets obtained are presented in Table 1. The training dataset was used for the adjustment of connection weights, while test dataset was used to determine the precision of both models. The validation dataset was used to prevent network overtraining in the case of BPNN, while in the case of GRNN it was used for the determination of the optimal smoothing factor (see section 2.4.). The ANN models were created using Neuroshell 2 software [36]. The architecture and training parameters of both ANN models are presented in Figure 2 and Table 2, respectively.

Table 2. ANNs training parameters

Training parameter	BPNN	GRNN
Scale function	Linear	Linear
Activation function	Sigmoid	Exponential
Learning algorithm (details)	Backpropagation (Learning rate=0.1, Momentum=0.1, Initial weights=0.3)	Genetic (Euclidean distance metric)
Termination	Automatic[a]	Automatic[b]

[a]after 100000 iterations with no improvement

[b]after 20 generations with no improvement of 1%

The results of the created models were analyzed using multiple performance metrics:

The correlation coefficient (r):
$$r = \frac{1}{n-1}\sum_{i=1}^{n}\frac{(c_o-\bar{c}_o)(c_p-\bar{c}_p)}{s_o s_p} \quad (6)$$

The root mean squared error (*RMSE*):
$$RMSE = \sqrt{\frac{1}{n}\left[(c_p-c_o)^2\right]} \quad (7)$$

The mean absolute error (*MAE)*:
$$MAE = \frac{1}{n}\sum_{i=1}^{n}\left|c_p-c_o\right| \quad (8)$$

Mean absolute percentage error (*MAPE*):
$$MAPE = \frac{1}{n}\sum_{i=1}^{n}\frac{\left|c_o-c_p\right|}{c_p}100(\%) \quad (9)$$

where C_o and C_p are the nominal and predicted concentrations, S_o and S_p are the standard deviation of nominal and predicted concentration, and the over bar refers to the average of the values.

The results obtained with these ANNs, for the simultaneous prediction of PBS and PCM in the test samples, are presented in Figure 10, while the values of corresponding performance metrics are presented in Table 3.

Table 3. Performance metrics of created ANN models

Performance metrics	PBS		PCM	
	BPNN	GRNN	BPNN	GRNN
R^2	0.98	0.93	0.98	1.00
r	0.99	0.96	0.99	1.00
RMSE[a]	0.16	0.33	1.98	1.81
MAE[a]	0.10	0.28	1.91	1.61
MAPE[b]	8.4	18.5	3.6	3.4

[a]expressed in μM

[b]expressed in %

It can be observed that the BPNN and GRNN were converged on rather different manner: the BPNN has predicted the concentration of both compounds with the similar high accuracy (MAPE values are in range 3.6–8.4%), while the GRNN has demonstrated considerably better prediction performance for the PCM (MAPE = 3.4%) in comparison with the PBS (MAPE = 18.5%).

Very high correlation coefficients (r = 0.99 ± 0.01) with regression lines close to the ideal regressions (R^2 = 0.99 ± 0.01) were obtained in all cases, except for the GRNN fit of PBS. Both models have demonstrated a greater precision for the PCM in comparison with the PBS. The prediction capability of the BPNN model could be considered satisfactory for the simultaneous determination of PBS and PCM.

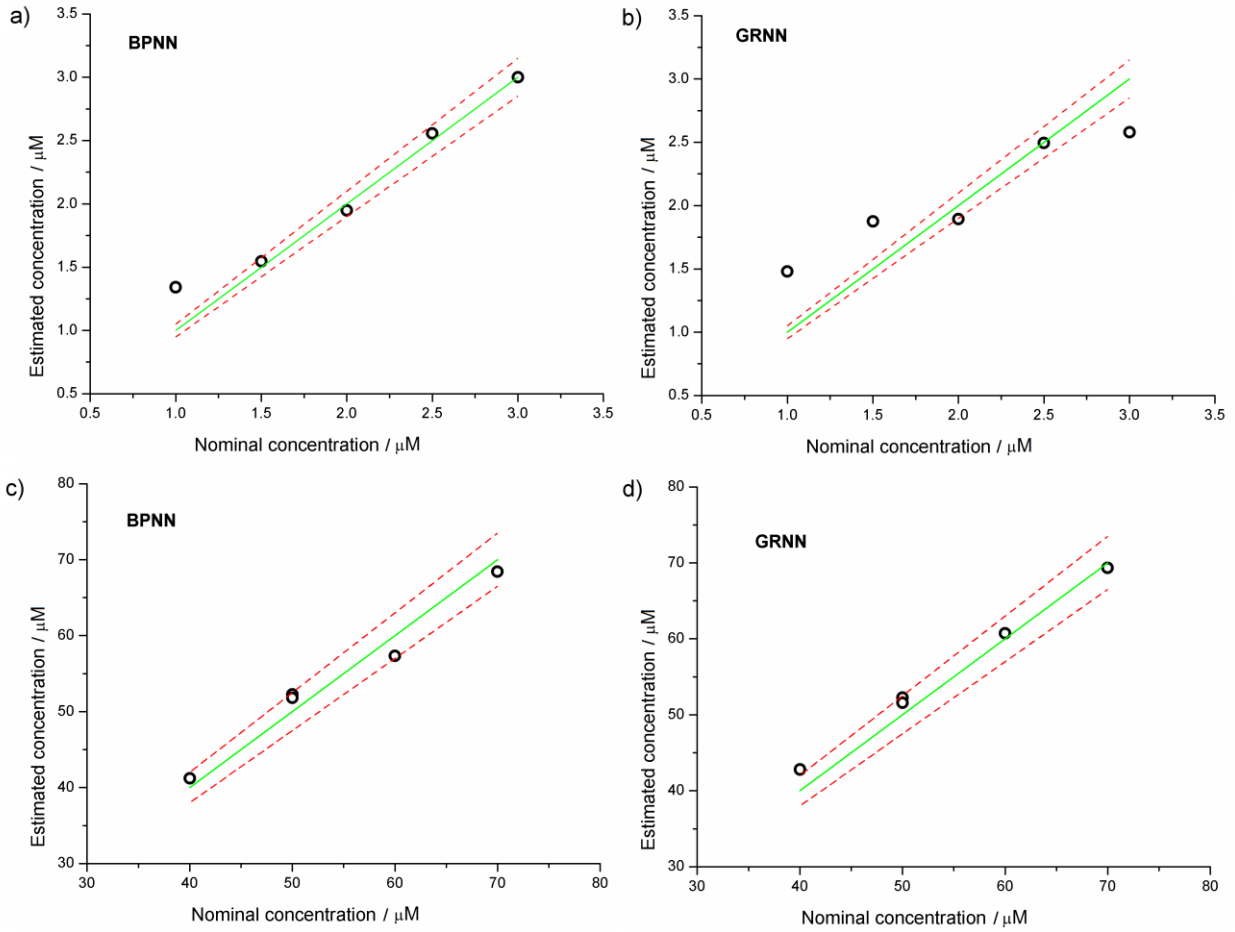

Figure 10. Comparison of the nominal and estimated concentrations for PBS a) BPNN b) GRNN and PCM c) BPNN d) GRNN. Solid lines represent the ideal regressions with the corresponding prediction error of 5% (dashed lines).

4. CONCLUSIONS

The voltammetric characterization and determination of PBS and PCM was performed by CV and SWV on gold electrode in a 0.05 M bicarbonate solution. A calibration curve of PBS, obtained by SWV has two linear ranges, from 1.0 μM to 3.0 μM and from 5.0 μM to 35.0 μM with a LOQ of 0.62 μM and LOD of 0.19 μM. The dominant peak of PCM enabled the construction of calibration curve

within the range from 10.0 to 50.0 μM with a LOQ of 8.53 μM and LOD of 2.56 μM. For the small peak of PCM, the calibration curve is obtained within the range from 30.0 to 100.0 μM. With the aid of chemometrics, the results obtained by SWV enabled the simultaneous determination of PBS and PCM. Two different ANN architectures have been successfully applied to the decomposition of the SWV peaks of the binary mixtures and the developed ANN models have been compared for the simultaneous prediction of the concentrations of PBS and PCM in a synthetic sample. Both models have demonstrated a greater precision for PCM in comparison with PBS.

The proposed SWV-ANN approach for the simultaneous determination of PBS and PCM is simple, inexpensive, precise and does not require any complex pretreatment. Because of this, we believe that it offers a new promising application of a bare gold electrode for the analytical purposes.

ACKNOWLEDGMENT
The work was supported by the Ministry of Education, Science and Technological Development of the Republic of Serbia (Projects No. ON172013, ON172060 and ON172007).

References

1. G.K. McEvoy, *AHFS Drug Information*, American Society of Health-System Pharmacists, Bethesda (1995)
2. B. Leduc, *Antiseisure agent*, in: T. Lemke, D. Williams (Eds.), *Foye's Princ. Med. Chem., 6th ed*., Lippincott Williams & Wilkins, Philadelphia, PA (2008) p. 533
3. G.M. Brenner, C.W. Stevens, *Pharmacology, 4th ed*., Sanders/Elsevier (2012)
4. J. Zhang, W.R. Heineman, H.B. Halsall, *J. Pharm. Biomed. Anal.* 19 (1999) 145
5. Steering Committee on Quality Improvement and Management, Subcommittee on Febrile Seizures, *Pediatrics*. 121 (2008) 1281
6. A. Bozdogan, G.K. Kunt, A. M. Acar, *Anal. Lett.* 25 (1992) 2051
7. Y. Ni, C. Liu, S. Kokot, *Anal. Chim. Acta.* 419 (2000) 185
8. J.T. Franeta, D. Agbaba, S. Eric, S. Pavkov, M. Aleksic, S. Vladimirov, *iI Farm.* 57 (2002) 709
9. Y. Ni, Y. Wang, S. Kokot, *Anal. Lett.* 37 (2004) 3219
10. J.B. Raoof, M. Baghayeri, R. Ojani, *Colloids Surf. B* 95 (2012) 121
11. E. Guo, *Int. J. Electrochem. Sci.* 10 (2015) 7341
12. F. Faridbod, M.R. Ganjali, P. Norouzi, *Int. J. Electrochem. Sci.* 4 (2009) 1679
13. X. Lü, Z. Wu, J. Shen, J. Feng, Y. Wang, Y. Song, *Int. J. Electrochem. Sci.* 8 (2013) 2229
14. M.B. Gholivand, M. Amiri, *J. Electroanal. Chem.* 676 (2012) 53
15. V.A. Pedrosa, D. Lowinsohn, M. Bertotti, *Electroanalysis* 18 (2006) 931
16. A.G. Cabanillas, M.I.R. Cáceres, M.A.M. Cañas, J.M.O. Burguillos, T.G. Díaz, *Talanta* 72 (2007) 932
17. G.K. Ziyatdinova, A.A. Saveliev, G.A. Evtugyn, H.C. Budnikov, *Electrochim. Acta.* 137 (2014) 114
18. E. Cukrowska, L. Trnková, R. Kizek, J. Havel, *J. Electroanal. Chem*. 503 (2001) 117
19. M.B. Gholivand, A.R. Jalalvand, H.C. Goicoechea, T. Skov, *Talanta* 119 (2014) 553
20. [P. Qiu, Y. Ni, S. Kokot, *J. Environ. Sci. Heal. Part B* 49 (2014) 722
21. A.Y. Tesio, S.N. Robledo, A.M. Granero, H. Fernández, M.A. Zon, *Sensors Actuators, B Chem.* 203 (2014) 655
22. N.P. Trišović, B.D. Božić, J.D. Lović, V.D. Vitnik, Ž.J. Vitnik, S.D. Petrović, M.L. Avramov Ivić, *Electrochim. Acta*. 161 (2015) 378

23. S.A. Kalogirou, *Prog. Energy Combust. Sci.* 29 (2003) 515
24. D.E. Rumelhart, G. Hinton, R. Williams, *Nature* 323 (1986) 534
25. D.F. Specht, *IEEE Trans. NEURAL NETWORKS.* 2 (1991) 568
26. A. Rentziou, K. Gkritza, R.R. Souleyrette, *Transp. Res. Part A Policy Pract.* 46 (2012) 487
27. D. Antanasijević, V. Pocajt, M. Ristić, A. Perić-Grujić, *Energy* 84 (2015) 816
28. Y.-H. Chen, F.-J. Chang, *J. Hydrol.* 367 (2009) 125
29. S. Kim, H.S. Kim, *J. Hydrol*. 351 (2008) 299
30. M.L. Avramov Ivić, S.D. Petrović, D.Ž. Mijin, *Contribution to the Recent Advances in Electrochemical Analysis of Pharmaceuticals*, in: Stojan S. Djokic (Ed.), *Modern Aspect of Electrochemistry,* Springer (2016) p. in press.
31. C.S. Santos, R. Mossanha, C.A. Pessôa, *J. Appl. Electrochem.* 45 (2015) 325
32. A.J. Bard, L.R. Faulkner, *Electrochemical methods: fundamentals and applications*, John Wiley & Sons, New York (2001)
33. E. Laviron, *J. Electroanal. Chem. Interfacial Electrochem.* 100 (1979) 263
34. J.N. Miller, J.C. Miller, *Statistics and Chemometrics for Analytical Chemistry, 4th ed.*, Pearson Education Limited, Essex, England (2000)
35. O. Benedito da Silva, S.A.S. Machado, *Anal. Methods.* 4 (2012) 2348
36. *Neuroshell 2 Release 4.2*, Ward systems group Inc., MD, USA (2007)